Saudi Pharmaceutical Journal 28 (2020) 729–736

Contents lists available at ScienceDirect

Saudi Pharmaceutical Journal

journal homepage: www.sciencedirect.com

Original article

Spectroscopic and molecular docking studies for characterizing binding mechanism and conformational changes of human serum albumin upon interaction with Telmisartan

Mohammed Al bratty

Department of Pharmaceutical Chemistry, College of Pharmacy, Jazan University, P. Box No. 114, Jazan, Saudi Arabia

ARTICLE INFO

Article history:
Received 18 March 2020
Accepted 28 April 2020
Available online 6 May 2020

Keywords:
Human serum albumin
Telmisartan
Binding
UV–Vis
FT-IR
Molecular Docking

ABSTRACT

Human serum albumin (HSA), one of the most copious plasma proteins is responsible for binding and transportation of many exogenous and endogenous ligands including drugs. In this study, we intended to explore the extent and types of binding interaction present between HSA and the antihypertensive drug, telmisartan (TLM). The conformational changes in HSA due to this binding were also studied using different spectroscopic and molecular docking techniques. The spectral shifting and intensity variations upon interaction with TLM were studied using FT-IR spectroscopy. Binding constant and the change in absorption of HSA at its λ_{max} was analyzed using absorption spectroscopy. Eventually, the types and extent of binding interactions were confirmed using molecular docking technique. Results have shown that TLM significantly interacts with the binding site-1 of HSA utilizing strong hydrogen bonding with Glu292, and Lys195 residues. The UV-absorption intensities were found to be decreased serially as the drug concentration increased with a binding constant of $1.01 \times 10^3\ M^{-1}$. The secondary structure analysis using FT-IR spectroscopy also revealed a marked reduction in the α-helix (56%) component of HSA on interaction. This study gives critical insights into the interaction of TLM with HSA protein which eventually affects the concentration of TLM reaching the site of action and ultimately its therapeutic profile.

1. Introduction

The Human Serum Albumin (HSA) is a negatively charged, highly soluble protein which is present in high concentration (60% of total protein) in plasma. Existence of several binding sites and an extraordinary binding capacity with a high degree of conformational flexibility makes HSA a versatile carrier to transport a variety of endogenous and exogenous ligands including drug molecules (Carter and Ho, 1994; Curry, 2009; Kratochwil et al., 2002; Sudlow, 1976). To date, two major binding sites namely site-1 and site-2 positioned in sub-domains IIA and IIIA respectively (Sudlow, 1976) and an additional binding site-3 (Zsila, 2013) positioned in sub-domain IB of HSA have been identified. The site-1 generally accommodates negatively-charged heterocyclic molecules, site-2 is known for its binding with negatively charged carboxylic acids and some acidic, basic as well as neutral molecules are shown to bind at site-3. However, several other molecules including indoxyl sulfate, ibuprofen (Ghuman, 2005), L-thyroxine (Petitpas, 2003) and dansyl-L-asparagine (Simard, 2006) are also shown to interact at these sites. Fig. 1 represents the three-dimensional (3-D) structure of HSA showing its three binding sites.

Telmisartan (TLM) is a non-peptide angiotensin II receptor (AT_1) blocker that acts by relaxing the smooth muscles of blood vessels and making blood easy to flow. It is used to treat hypertension and thereby, assists in the prophylaxis of strokes, heart attacks as well as kidney-related issues. Chemically, it is 4′-(1-methyl-2′-propyl-1*H*- [2,5′] bibenzoimidazolyl-3′-ylmethyl) biphenyl-2-carboxylic acid with a molecular weight of 514.63 (Fig. 2).

Telmisartan binds to plasma proteins significantly (>99.5%) mainly to albumin and to some extent α_1-acid glycoprotein, and

Abbreviations: HAS, Human Serum Albumin; TLM, Telmisartan; λ_{max}, wavelength of maximum absorbance; Glu, Glutamate; Lys, Lysine; ADME, Absorption, Distribution, Metabolism, Excretion; UCSF, University of California, San Fransisco; PDB, Protein Data Bank.

Peer review under responsibility of King Saud University.

Production and hosting by Elsevier

E-mail address: malbratty@jazanu.edu.sa

https://doi.org/10.1016/j.jsps.2020.04.015
1319-0164/

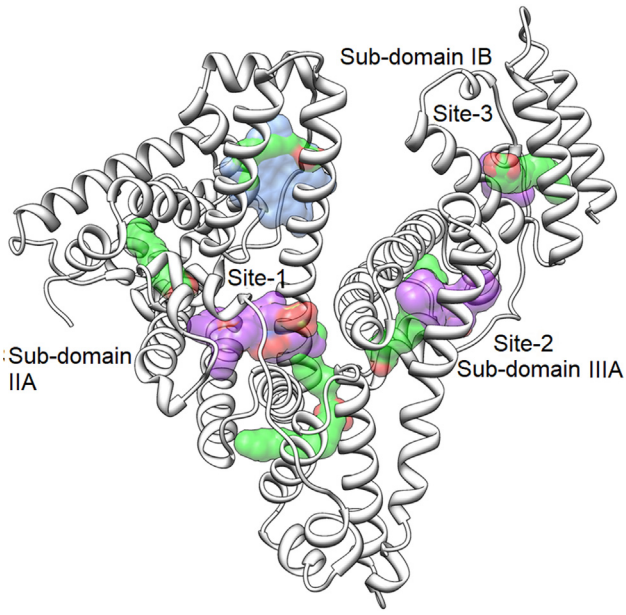

Fig. 1. 3-D structure of HSA protein showing the three major binding sites.

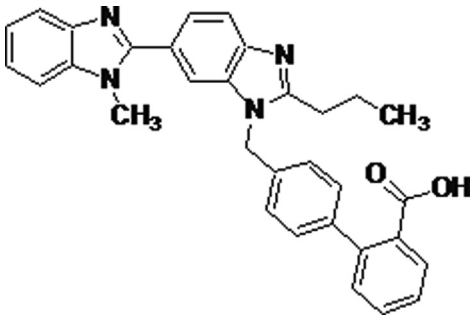

Fig. 2. Structure of Telmisartan.

remains unchanged over different concentration ranges and doses of the drug. It also shows a very high volume of distribution of approximately 500 L which indicates additional tissue binding. Interaction of various drug molecules to HSA is of important concern as the strong binding affects the pharmacokinetic parameters, particularly the distribution volume and clearance rate of the drug. This binding gets the drugs sequestered making it less available to bind to its target (Reichel, 2009). Besides, it is equally important for the drugs which cross the blood-brain barrier (BBB), as only the unbound portion would remain available to diffuse and reach the brain (Howard et al., 2010). Overall, binding to HSA changes the ADME profile of small molecules and the optimization of this interaction is used in drug discovery and development to come up with new therapeutic agents (Kratz and Elsadek, 2012). The therapeutic effectiveness of a drug molecule is influenced by its protein binding ability; in addition to that, it also affects toxicity and drug stability during the therapeutic processes. The binding ability of a drug molecule with plasma protein is one of the main factors that affect the diffusion from the circulatory system and hence bioavailability. Therefore, it is important to assess the types and extent of binding interactions between drugs and HSA. Recently High-performance affinity chromatography (HPAC) (Ryan et al., 2015), Nuclear Magnetic Resonance (NMR) spectroscopy (Rieko, 2015) have been employed for studying drug-protein interactions. However, these techniques are costly, require much expertise and are associated with complex procedures and therefore, cannot be used for routine purposes. The FT-IR and UV spectroscopic techniques are advantageous over other techniques in being easy to perform and are cost-effective (Malik et al., 2017; Nasser et al., 2020).

In a recent study, the interaction of TLM with bovine serum albumin (BSA) has been reported using FT-IR, UV, Fluorescence spectroscopy, and molecular docking (Zhou et al., 2019). In this study, the binding of TLM with HSA was explored using FT-IR and UV–Visible spectroscopy and the results obtained were confirmed with molecular docking technique.

2. Materials and methods

2.1. Chemicals and instruments

Lyophilized Human Serum Albumin powder (HSA, 99%), Telmisartan drug (>99% pure), sodium phosphate dibasic and sodium phosphate monobasic-anhydrous were purchased from Sigma-Aldrich, Saint Louis, USA. The double-distilled ultrapure water was prepared in our lab. FT-IR spectrophotometer (Nicolet iS10, Thermo Fischer Scientific, USA) was used for FT-IR spectroscopic analysis, whereas UV–Vis spectroscopic analysis was performed on a double beam UV–Visible Spectrophotometer (Shimadzu, Japan). Molecular docking studies were carried out using UCSF Chimera 1.13.1 integrated with AutoDock Vina 1.1.2 software (California University, San Francisco, USA).

2.2. Preparation of stock solutions of drug and protein

Phosphate buffer (0.1 M) containing 0.05 M sodium chloride was prepared using ultrapure water and the pH of the final solution was maintained to 7.2 using 0.2 M NaOH. The protein stock solution (0.6 mM) was prepared using the same buffer by dissolving 40 mg of lyophilized HSA powder per mL of buffer. A stock solution of TLM (1 mM) was prepared by dissolving accurately weighed 51.46 mg TLM powder in 100 mL of freshly prepared phosphate buffer added in portions along with 500 μL of dimethyl sulfoxide to increase the solubility of TLM. The final concentration of DMSO in the measured samples for FTIR studies was $\leq$0.25% v/v and for UV studies the final concentration was $\leq$0.016% v/v.

2.3. FT-IR spectroscopic analysis

2.3.1. Methodology

Telmisartan and HSA solutions were mixed properly in equal volumes to get the final protein concentration (0.3 mM) and two drug concentrations (0.1 and 0.5 mM). Hydrated films of samples were prepared to record the FT-IR spectra after incubation of HSA with both drug concentrations separately at room temperature (25 ± 2 °C) for 2 h. Protein-drug complexes spectra were taken at 4 cm^{-1} resolution and 100 scans were made over 4000–400 cm^{-1} transmittance range. A difference spectrum was obtained by subtracting the protein alone spectrum from the spectra of drug-protein complexes (Dousseau et al., 1989).

2.3.2. Conformational analysis of HSA

Upon interaction with different drug concentrations, spectral shifting and intensity variations of the amide-A band (NH_{str} at 3500 cm^{-1}), the amide-I band (mainly C = O_{str} at 1660–1650 cm^{-1}), and amide-II band (C-N_{str} coupled with NH-bending at 1550 cm^{-1}) of HSA protein were studied. The shape of the amide-I band at 1600–1650 cm^{-1} was also used to study the secondary structure of the protein (Byler and Susi, 1986). Second derivative resolution enhancement and Fourier self deconvolution were also performed using OriginPro software to enhance the spec-

tral resolution over 1700–1600 cm^{-1} range. Gaussian line shape was set in between the spectral range of 1700–1600 cm^{-1} through the least square curve-fitting method. Characteristic peaks of α-helix (at 1660–1649 cm^{-1}), random coil (at 1648–1641 cm^{-1}), β-sheet (at 1640–1615 cm^{-1}), β-turn (at 1680–1660 cm^{-1}), and β-antiparallel (at 1692–1680 cm^{-1}) components were set and their area were calculated using Gaussian functions. The total area of the amide-I band was calculated by adding all the above peak areas. Percentages of Amide I components were obtained by dividing the area of each peak by total area (Ahmed et al., 1995).

2.4. UV–Vis spectroscopic analysis

The UV–Visible spectroscopic studies were performed according to the method described earlier (Stephanos, 1996; Zhong et al., 2004) with slight modification. Accurately weighed amounts of HSA and TLM were dissolved separately in phosphate buffer (0.1 M, pH 7.2) to achieve stock solutions of 0.6 mM and 1 mM concentrations respectively. A working solution of HSA showing optimum absorbance was selected to examine the complexation between the protein and TLM. Subsequently, various working solutions were made by mixing the protein and drug stock solution, where the measured amounts of drug solution were added to achieve concentrations of 0, 4, 8, 12, 16, 20, 24, 28 and 32 μM for TLM, while the concentration of protein was kept constant at 12 μM in all solutions. The final volume of all the working solutions was made up to 5 mL using phosphate buffer (0.1 M, pH 7.2) and kept constant for all samples. The solutions were gently mixed by vortex shaker and incubated at room temperature (25 ± 2 °C) for 2 h with occasional shaking. The absorption spectrum of HSA alone and HSA-TLM complex was obtained over the wavelength range of 200–400 nm. Complexation between HSA and TLM was investigated by monitoring the absorbance at 278 nm. To avoid interference due to TLM absorption at 278 nm, the spectra were corrected by subtracting the TLM absorption from that of HSA-TLM adduct before determining the binding constant of the drug-protein complex.

2.5. Molecular docking studies

Telmisartan was docked separately to the binding site-1 and site-2 corresponding to subdomain-IIa and IIIa respectively (Russell et al., 2016; Tayyab et al., 2019). UCSF Chimera 1.13.1 integrated with AutoDock Vina 1.1.2 software was used for docking Huang et al., 2014, Trott and Olson, 2010). The 3D structures of HSA were taken from the RCSB protein data bank using the PDB IDs: site 1 (PDB ID: 2BXB, resolution: 3.2 Å) and site 2 (PDB ID: 2BXF, resolution: 2.95 Å). The 3D structure of TLM was loaded to the Chimera window through its PubChem ID (CID: 65999). The Dock Prep mode in Chimera was used to prepare the HSA before docking. The monomer chain A was retained and solvent molecules were deleted. Subsequently, polar hydrogens were added and the Gasteiger charges were calculated to make it ready for docking. The structure of TLM was optimized for its geometry, charges and atom energy by applying AMBER force field, the addition of hydrogens, and Gasteiger charges. The TLM molecule possesses eight rotatable bonds and all of them were set active. Eventually, the flexible TLM structure was docked to the protein which was made rigid. Docking analysis of TLM with the binding sites of HSA was executed using the plug-in of AutoDock Vina. The binding site 1 was identified using native ligand and the grid box was generated with coordinates, x = 5, y = 9, and z = 9 Å and site 2 was located with coordinates, x = 12, y = 6, and z = 18 Å. A blind docking to ascertain the possible binding to site-3 was also performed by covering the unbound HSA (1BM0) with a grid box of size 60X60X60 centred at × = 25, y = 15, and z = 25 Å. The native ligands were deleted from 2BXB and 2BXF before docking and the conformations were searched with binding parameters of 3 kcal/mol as the maximum energy difference, 8 as exhaustiveness of search and 10 as the number of binding modes. Redocking of the native ligands with a root mean square deviation (RMSD) of 2 Å was the validation protocol applied. The docking scores by AutoDock Vina were used to grade the conformations in the order of their ΔG in kcal/mol, RMSD, and the number of hydrogen bonds. Discovery Studio 2016 software was utilized to study the best binding mode/conformation of TLM with HSA.

3. Theory and calculations

Binding constant, '*K*' was calculated using the absorbance data for HSA before and after complexation with TLM (Stephanos, 1996; Zhong et al., 2004). If we assume only one type of interaction exists between TLM and HSA in the aqueous solution and considering the total ligand $[TLM]_{total}$ concentration for indirect binding measurement, the following equations can be established:

$$HSA + TLM \iff HSA : TLM \tag{1}$$

$$[TLM]_f = [TLM]_{total} - [HSA : TLM] \tag{2}$$

$$[HSA]_{total} = [HSA : TLM] + [HSA] \tag{3}$$

$$[HSA] = \frac{[HSA : TLM]}{K \times [TLM]_f} \tag{4}$$

where $[TLM]_f$ is the concentration of unbound/free TLM and $[TLM]_{total}$ and $[HSA]_{total}$ are the concentrations of total TLM and total HSA added. 'K' is the association or binding constant for *HSA:TLM* complexes.

If we substitute Eq. (2) into (4) and Eq. (4) into (3), it would give the following equation:

$$[HSA]_{total} = [HSA : TLM] + \frac{[HSA : TLM]}{K\left([TLM]_{total} - [HSA : TLM]\right)} \tag{5}$$

If we consider the *[HSA : IRB]* as C_B, $[HSA]_{total}$ as C_{HSA} and $[TLM]_{total}$ as C_{TLM}, the equation will change to

$$C_{HSA} = C_B + \frac{C_B}{K \times (C_{TLM} - C_B)} \tag{6}$$

From Eq. (6), the value of '*K*' can be calculated as:

$$K = \frac{C_B}{(C_{HSA} - C_B) \times (C_{TLM} - C_B)} \tag{7}$$

As per the Beer-Lambert law:

$$C_{HSA} = \frac{A_0}{\varepsilon_{HSA} \cdot \ell} \tag{8}$$

$$C_B = \frac{(A_0 - A)}{\varepsilon_B \cdot \ell} \tag{9}$$

where A_0 and A are the absorbance of HSA in the absence and presence of TLM at 278 nm wavelength respectively, ε_{HSA} and ε_B are the molar extinction coefficients of HSA and the bound TLM respectively, whereas, ℓ is the path length and was considered as 1 cm.

Now, in Eq. (7), if we substitute the values of C_{HSA} and C_B from Eqs. (8) and (9), Eq. (10) can be deduced as follows:

$$\frac{A_0}{A_0 - A} = \frac{\varepsilon_{HSA}}{\varepsilon_B} + \frac{\varepsilon_{HSA}}{\varepsilon_B \cdot K} \cdot \frac{1}{C_{TLM}} \tag{10}$$

By using this equation, a double reciprocal plot was drawn between $\frac{1}{A_0 - A}$ on Y-axis, and $\frac{1}{C_{TLM}}$on X-axis, which was obtained to be linear. The slope and intercept were obtained from the plot and the binding constant (K) was calculated as the ratio of intercept to the slope of the plot.

4. Results and discussion

4.1. FT-IR spectroscopic studies

FT-IR technique was utilized to study the binding of HSA with the drug solutions. On complexation of TLM at 0.5 mM concentration with HSA protein, a significant decrease in intensity of amide-I band (1655 cm^{-1}, free HSA, Fig. 3, Curve A) and amide-II band (1543 cm^{-1}, free HSA) was observed in the spectra of HSA-TLM complex (Fig. 3, Curve B). The negative peaks found in the difference spectra of amide-I and amide-II bands at 1658, 1542 cm^{-1} were due to the decrease in intensities of these bands (Fig. 3, Curve C). The intensity changes were observed due to the hydrogen bond interactions between drug and C═O, N—H and C—N groups of protein (Yang et al., 2012).

However, at lower drug concentration (0.1 mM), a relatively smaller change in transmittance was noticed upon complexation with HSA (Fig. 3, Curve D). The interaction of TLM with the C—N functional group of protein was also signified from the amide-A band shifting to a higher wavenumber (3300 cm^{-1} to 3465 cm^{-1}). Besides, shifting of the amide-I band from 1655 cm^{-1} (free HSA) to 1658 cm^{-1} as well as an amide-II band from 1543 cm^{-1} (free HSA) to 1542 cm^{-1} (Fig. 3, Curve B) was also observed upon interaction. Shifting of amide-I and amide-II bands occurred due to H-bonding between the TLM and C═O and C—N functional groups of HSA. The reduction in the amide-I band was additionally identified by the decrease in the α– helix component of the protein. The secondary structure of HSA protein was quantitatively analyzed through the curve fitting method and the results are summarized in Table 1 and Fig. 4. The secondary structures of amide 1 band of free HSA through curve fitting method showed the presence of α-helix (55%), β-turn (17%), β-sheet (13%), random coil (5%) and β-antiparallel (10%) components, which were found to be comparable with the reported HSA spectroscopic analysis (Beauchemin et al., 2007; Froehlich et al., 2009). As evident from Table 1 and Fig. 4 that upon interaction with TLM, the α-helix portion and the β-antiparallel component of HSA protein was significantly decreased from 55% to 24% and 10% to 4% respectively, whereas, β-turn, β-sheet, and random coil were observed to be increased from 17% to 31%, 13% to 21%, and 5% to 20%, respectively. A substantial reduction in the intensity of the amide-I band observed at higher drug concentration (0.5 mM) was because of the loss of α-helix content in HSA. A marked reduction in α-helix and augmentation of other components (except β-antiparallel) of the HSA secondary structure relates to the partial unfolding of the protein upon drug interaction.

4.2. UV–Visible spectroscopic analysis

The consequence of increasing concentrations of TLM on the UV spectrum of HSA was studied using absorption spectroscopy. Maximum absorbance with a strong absorption peak at 278 nm was monitored and the results showed that the peak intensity was linearly decreased with increasing concentrations of TLM (Fig. 5). The obvious reduction in the absorption intensity of HSA indicated the formation of the complex between HSA and TLM as well as the conformational alterations in the structure of protein on interaction.

The strong absorption peak in the UV spectrum of HSA at 278 nm was due to the presence of aromatic moieties of phenylalanine, tyrosine and tryptophan residues. The reduction in the absorption intensity at this region may be attributed to the

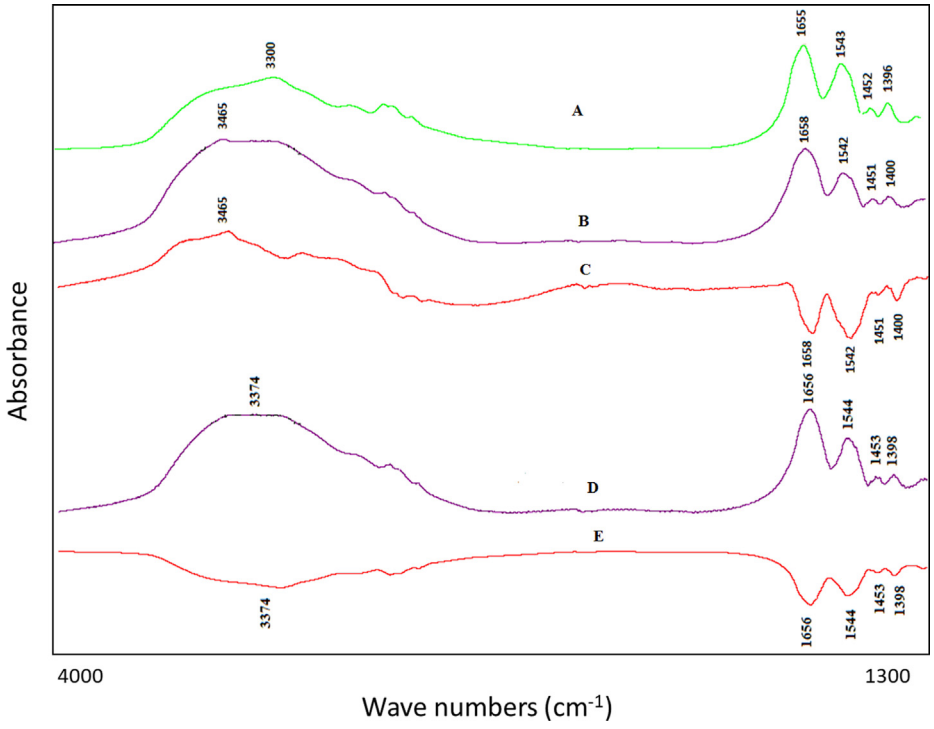

Fig. 3. FT-IR spectra and difference spectrum [(HSA + TLM) – (Free HSA)] over the region 4000–1300 cm^{-1} for HSA alone and HSA-TLM complexes with different drug concentrations (0.1 mM and 0.5 mM) and final HSA concentration 0.3 mM. (A) HSA alone; (B) HSA-TLM complex (0.5 mM); C) Difference spectrum of HSA-TLM complex (0.5 mM); (D) HSA-TLM complex (0.1 mM); (E) Difference spectrum of HSA-TLM complex (0.1 mM).

Table 1
Determination of secondary structure for HSA alone (0.3 mM) and HSA-TLM complex (0.5 mM) at physiological pH and room temperature.

Amide I (cm^{-1}) components	Free HSA (%) 0.3 mM	HSA-TLM complex (%)*
β –sheet (±2) 1640–1615	13	21
Random coil (±2) 1648–1641	05	20
α –helix (±4) 1660–1649	**55**	24 (−56.36%)**
β- turn (±2) 1680–1660	17	31
β –antiparallel (±1) 1692–1680	10	04

* Concentration of TLM in HSA-TLM complex = 0.5 mM.
** Percentage variation in HSA α-helix after its drug complexation.

hydrophobic interaction between aromatic regions of the drug and protein molecules, which may have resulted in the unfolding of protein backbone as well as a reduction in the hydrophobicity of the protein microenvironment (Naik et al., 2015; Suryawanshi et al., 2016).

To determine the binding constant between TLM and HSA, a double-reciprocal plot (Fig. 6) of $1/(A_0 - A)$ vs. $1/C_{TLM}$ was constructed, which resulted in a straight trend line, indicating a linear relationship ($R^2 > 0.9$). The 'A_0' represents the absorbance of HSA solution in absence of TLM, 'A' denotes the absorbances of HSA-TLM complexes at different drug concentrations and C_{TLM} is the concentration of TLM in the protein-drug complex. The binding constant (K) for the present drug-protein interaction was calculated by dividing intercept with the slope of the double reciprocal plot and found to be 1.01×10^3 M^{-1}, which indicated a moderate affinity of drug with HSA at physiological pH.

The therapeutic effectiveness of a drug molecule is influenced by its protein binding ability; in addition to that, it also affects toxicity and drug stability during the therapeutic processes. Studying *in-vitro* protein-drug complexation is considered as an effective method for getting insight into the actual protein-drug interaction in the biological system. Measurement of UV absorption is considered to be an accurate and simple tool to study the complex formation between the protein and ligand molecules. The UV spectrum has also been used to understand the structural changes after ligand binding (Pan et al., 2011; Valeur, 2001).

The binding ability of a drug molecule with plasma protein is one of the main factors that affect the diffusion from the circulatory system and hence bioavailability. Most therapeutic agents bind reversibly to the plasma protein and exhibit moderate binding strength. A drug will be poorly distributed and will have short half-life due to rapid metabolism and elimination if it exhibits weak binding interaction with plasma protein. However, too strong affinity may also result in the reduction of free drug concentration in blood plasma which is required to produce the desired level of therapeutic action (Colmenarejo et al., 2001; Dufour and Dangles, 2004). The binding results in this study indicated that TLM effectively binds to HSA protein and is transported in the biological system.

4.3. Molecular docking studies

Three structurally homologous domains, namely Domains I, II and III are present in the stabilized secondary structure of HSA (Naik et al., 2015). Drugs are shown to fill and interact with the hydrophobic space at site-1, site-2, and site-3 (Nusrat et al., 2016). Several Angiotensin II-receptor blockers have been proved to interact with the serum albumin through binding to site-1 and site-2 (Alanazi et al., 2018; Li et al., 2010). Therefore, the docking method was used to explore the suitable binding site for TLM and to predict the proper binding conformation.

TLM was able to bind the site-1 of HSA (Fig. 7) with a binding energy of −9.6 kcal/mol, RMSD = 0, and it interacted through three hydrogen bonds. The Glutamic acid292 residue of HSA exhibited a hydrogen bond with a predicted bond length of 2.26 Å. The Lysine195 residue also formed two hydrogen bonds with TLM, whose bond lengths predicted as 2.35 and 2.79 Å. The —OH of carboxylic acid group of TLM was involved in the polar hydrogen contacts, —O— acts as a hydrogen bond acceptor (HBA), and the hydrogen atom of —OH acts as a hydrogen bond donor (HBD).

The polar and non-polar binding interactions of TLM with site-1 of HSA are represented in 3D and 2D views in Fig. 8A, B and C, prepared using Discovery Studio 2016. The 3D interaction diagram, Fig. 8A shows seven hydrophobic interactions, among which three interactions were considered significant given their inter-atomic distances of 4.37–4.85 Å, which occurred with Lys195, Trp214, and Val455. As evident from Fig. 8B, TLM was able to occupy the hydrophobic pocket of the site-1 of HSA. The hydrophobic residues surrounding the site-1, involved in the interaction with TLM were Ala191, Ala194, Trp214, Lys436, Tyr452, and Val455. Four significant alkyl interactions (bond lengths = 3.79–4.54 Å) were also pre-

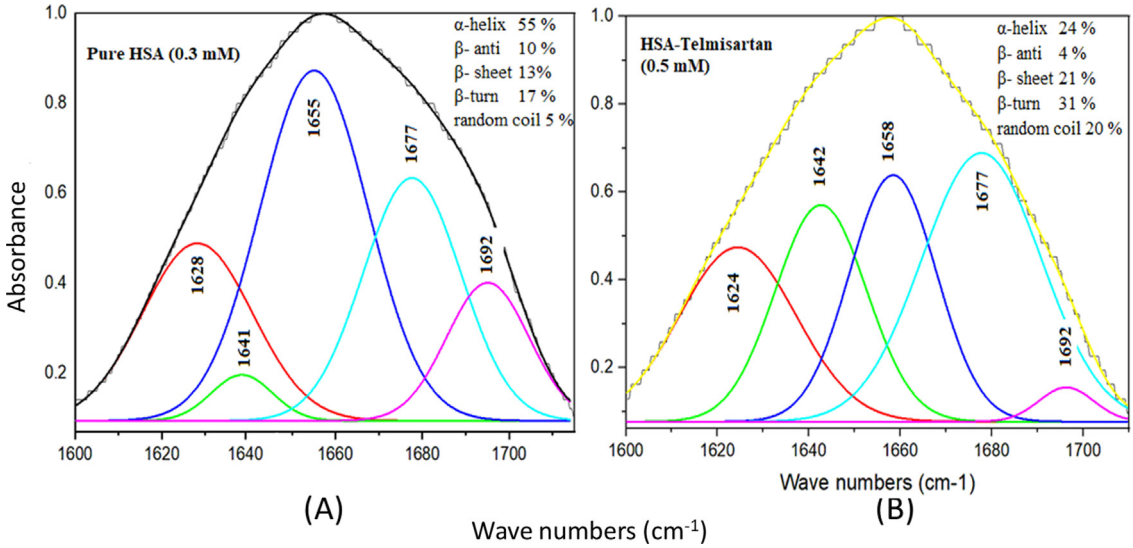

Fig. 4. Curve fitted amide (1700–1600 cm^{-1}) for HSA alone (A) and HSA-TLM complex (B) in phosphate buffer with 0.5 mM drug and 0.3 mM HSA concentrations.

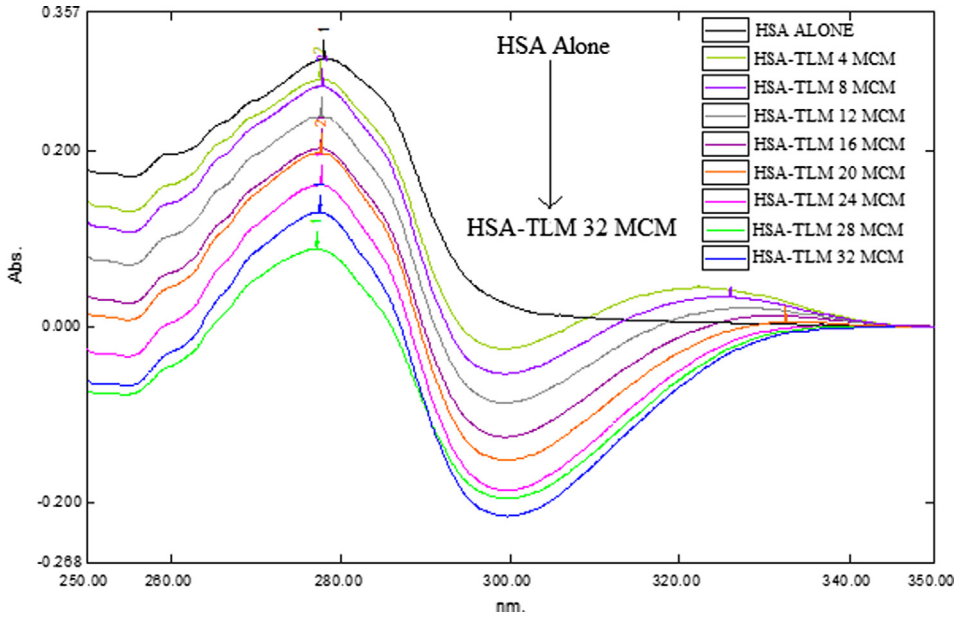

Fig. 5. Spectral overlay showing the effect of increasing concentrations of TLM on UV absorption of HSA. C_{HSA} = 12 μM; C_{TLM} = 0, 4, 8, 12, 16, 20, 24, 28 and 32 μM. Buffer: Sodium phosphate (pH 7.2).

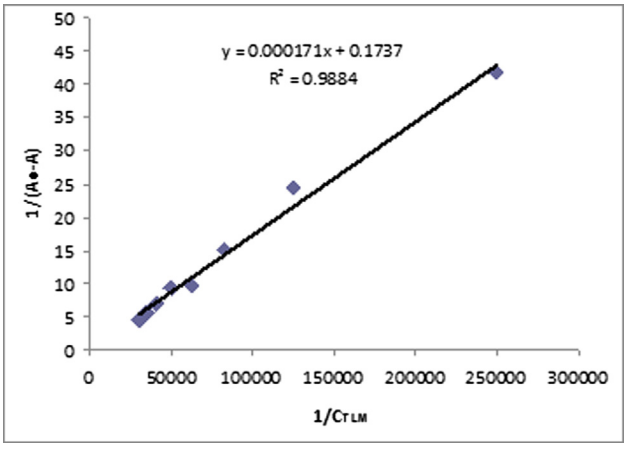

Fig. 6. The plot of $1/(A_0\text{-}A)$ vs. $1/C_{TLM}$; A_0 and A = absorbances of HSA alone and HSA-TLM complex; C_{TLM} = TLM concentration. C_{HSA} = 12 μM; C_{TLM} = 0, 4, 8, 12, 16, 20, 24, 28 and 32 μM; Buffer: Sodium phosphate (pH 7.2); Binding constant: 1.01 × 10^3 M^{-1}.

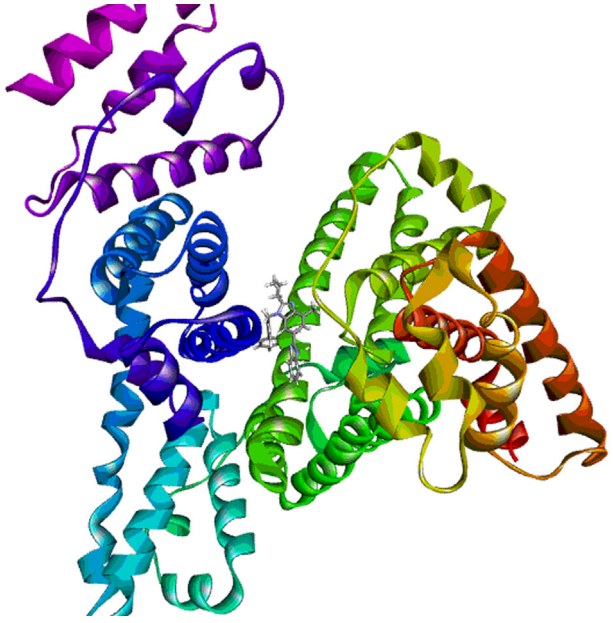

Fig. 7. Telmisartan bound to the site-1 of HSA. HSA is represented using ribbons in rainbow colors and TLM is shown in stick model.

dicted one each with Ala191, Ala194, Lys195, and Val455. Three Electrostatic π-cation interactions with Lys195 and two similar interactions with Arg218 were predicted at a distance less than 5 Å as shown in Fig. 8C. One π-anion interaction with Glu292 at a distance of 4.82 Å was also predicted. The Trp214 residue was present at a distance of 4.17 Å from one of the alkyl groups of TLM. The basic amino acid Lys195 interacted in its cationic form with TLM. The interaction of TLM with Lys195 stipulated that Lys195 plays a crucial role in the binding of TLM with HSA due to its imperative contacts established. The electrostatic and hydrophobic interactions were weaker than the hydrogen bonds, hence it is concluded that hydrogen bonds play an important role in stabilizing the interaction of TLM with HSA.

Molecular docking results indicated that TLM failed to interact with site-2 and site-3 of HSA. No hydrogen bonds were observed when TLM was docked to site-2 of HSA. Blind docking also predicted that TLM interacts with site 1 and not with site-2 or site-3.

Shifting of amide bonds and a decrease in α-helix content of HSA due to interaction of TLM, determined by FT-IR can be correlated to the hydrogen bonds predicted by molecular docking. The reduction in the intensity of UV absorption at 278 nm may be correlated to the hydrophobic interactions of TLM with the aromatic residues Trp214 and Tyr452 of sub-domain IIA of HSA. Results of FT-IR, UV spectroscopy, and docking studies on TLM binding to HSA correlated well and serve as a proof for the binding mechanism.

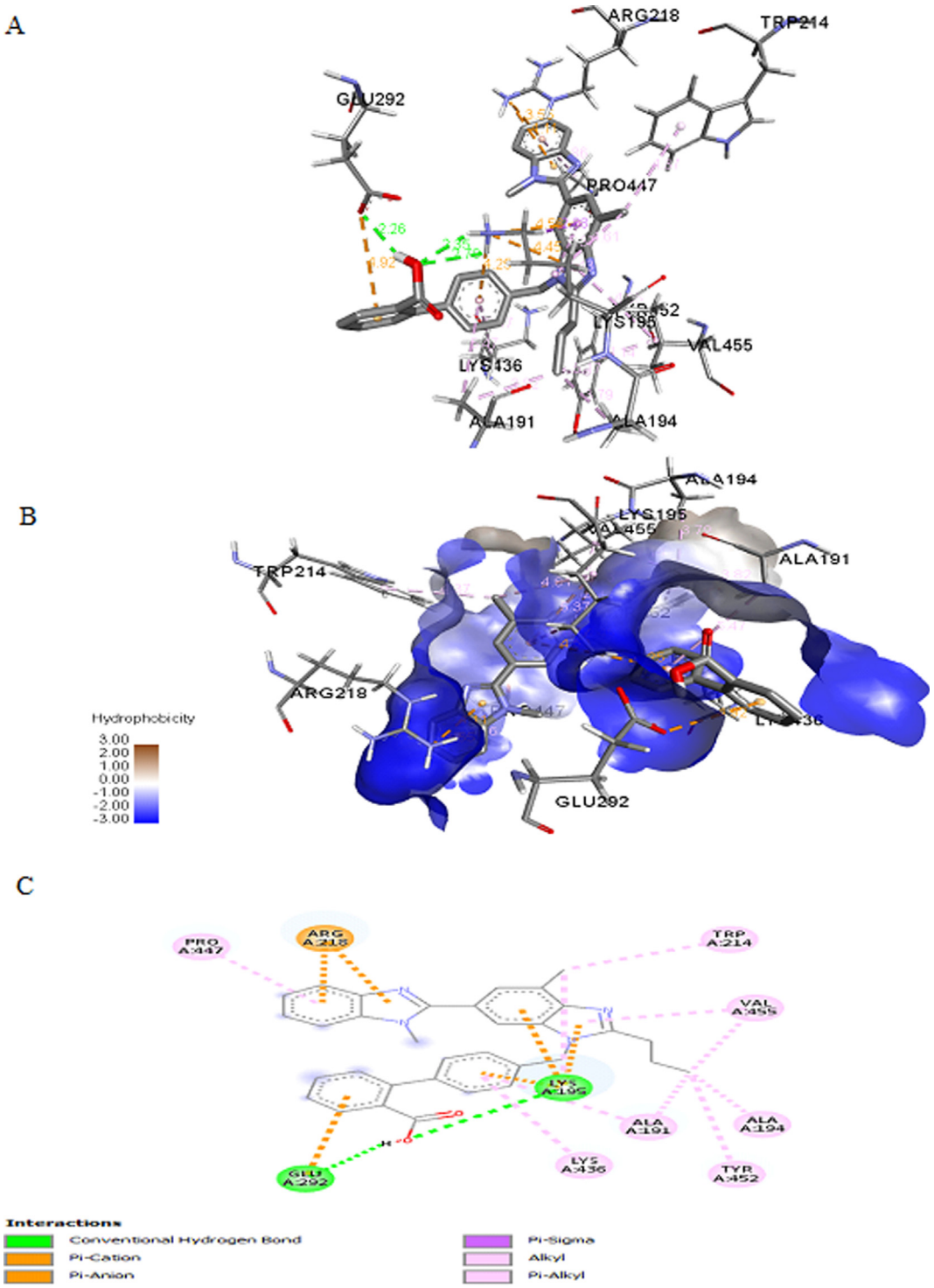

Fig. 8. (A) 3D representation of interactions of Telmisartan with the residues of site-1 of HSA (B) Telmisartan occupies the hydrophobic binding pocket of HSA (C) 2D interaction diagram showing the polar and hydrophobic interactions of Telmisartan with HSA. In A and B, TLM is represented as sticks colored by element and the residues are labeled and shown as thin sticks. In C, lines show the position of TLM, and discs are the interacting amino acids of HSA.

5. Conclusions

The binding interactions of TLM with HSA were successfully studied using two simple, easy to perform and cost-effective spectroscopic techniques, FT-IR and UV–Vis, which can be applied to study the binding interactions of other drug molecules with proteins on a routine basis. These spectroscopic techniques revealed the number and types of interactions between the drug and protein as well as the conformational changes in the protein upon binding. Binding with TLM resulted in a marked change in the conformation of HSA which was evident from the spectral shifting and intensity variations in FT-IR spectroscopy. It was quantified using secondary structure analysis of protein which showed a considerable change in the secondary structure components. The UV–Vis spectroscopy showed a linear decrease in the absorbance of HSA at 278 nm with an increase in the TLM concentration. Additionally, the binding

was confirmed using molecular docking studies which revealed the binding site of TLM, type of bonding as well as the residues and functional groups involved in the binding. TLM binds exclusively to site I of HSA through three strong hydrogen bonds which are the primary forces stabilizing the interaction. The Lys195 of the site-1 contributed to the majority of the binding interactions of HSA with TLM. Collectively, the results of the study correlated well and provide evidence for the characteristics of binding of TLM with HSA.

Funding

No grant was received for this study.

Declaration of Competing Interest

The authors declare that they have no known competing financial interests or personal relationships that could have appeared to influence the work reported in this paper.

References

Ahmed, A., Tajmir-Riahi, H.A., Carpentier, R.A., 1995. Quantitative secondary structure analysis of the 33 kDa extrinsic polypeptide of photosystem II by FT-IR spectroscopy. FEBS Lett. 363, 65–68. https://doi.org/10.1016/0014-5793(95)00282-e.

Alanazi, A.M., Abdelhameed, A.S., Bakheit, A.H., Hassan, E.S., Almutairi, M.S., Darwish, H.W., Attia, M.I., 2018. Spectroscopic and molecular docking studies of the binding of the angiotensin II receptor blockers (ARBs) azilsartan, eprosartan and olmesartan to bovine serum albumin. J. Lumin. 203, 616–628. https://doi.org/10.1016/j.jlumin.2018.06.085.

Byler, D.M., Susi, H., 1986. Examination of the secondary structure of proteins by deconvoluted FT-IR spectra. Biopolymers 25, 469–487. https://doi.org/10.1002/bip.360250307.

Beauchemin, R., N'soukpoe-Kossi, C.N., Thomas, T.J., Thomas, T., Carpentier, R., Tajmir-Riahi, H.A., 2007. Polyamine analogues bind human serum albumin. Biomacromolecules 8, 3177–3183. https://doi.org/10.1021/bm700697a.

Carter, D.C., Ho, J.X., 1994. Structure of serum albumin. Adv. Protein Chem. 45, 153–203. https://doi.org/10.1016/S0065-3233(08)60640-3.

Colmenarejo, G., Alvarez-Pedraglio, A., Lavandera, J.L., 2001. Cheminformatic models to predict binding affinities to human serum albumin. J. Med. Chem. 44, 4370–4378. https://doi.org/10.1021/jm010960b.

Curry, S., 2009. Lessons from the crystallographic analysis of small molecule binding to human serum albumin. Drug Metab. Pharmacokinet. 24, 342–357. https://doi.org/10.2133/dmpk.24.342.

Dousseau, F., Therrien, M., Pezolet, M., 1989. On the spectral subtraction of water from the FT-IR spectra of aqueous solutions of proteins. Appl. Spectrosc. 43, 538–542.

Dufour, C., Dangles, O., 2004. Flavonoid-serum albumin complexation: determination of binding constants and binding sites by fluorescence spectroscopy. BBA 1721, 164–173. https://doi.org/10.1016/j.bbagen.2004.10.013.

Froehlich, E., Jennings, J.C., Sedaghat-Herati, M.R., Tajmir-Riahi, H.A., 2009. Dendrimers bind human serum albumin. J. Phys. Chem. B 113, 6986–6993. https://doi.org/10.1021/jp9011119.

Ghuman, J., Zunszain, P.A., Petitpas, I., Bhattacharya, A.A., Otagiri, M., Curry, S., 2005. Structural basis of the drug-binding specificity of human serum albumin. J. Mol. Biol. 353, 38–52. https://doi.org/10.1016/j.jmb.2005.07.075.

Howard, M.L., Hill, J.J., Galluppi, G.R., McLean, M.A., 2010. Plasma protein binding in drug discovery and development. Comb. Chem. High Throughput Screen. 13, 170–187. https://doi.org/10.2174/138620710790596745.

Huang, C.C., Meng, E.C., Morris, J.H., Pettersen, E.F., Ferrin, T.E., 2014. Enhancing UCSF Chimera through web services. Nucleic Acids Res. 42, W478–W484. https://doi.org/10.1093/nar/gku377.

Kratochwil, N.A., Huber, W., Müller, F., Kansy, M., Gerber, P.R., 2002. Predicting plasma protein binding of drugs: a new approach. Biochem. Pharmacol. 64, 1355–1374. https://doi.org/10.1016/s0006-2952(02)01074-2.

Kratz, F., Elsadek, B., 2012. Clinical impact of serum proteins on drug delivery. J. Control. Release 161, 429–445. https://doi.org/10.1016/j.jconrel.2011.11.028.

Li, J., Zhu, X., Yang, C., Shi, R., 2010. Characterization of the binding of angiotensin II receptor blockers to human serum albumin using docking and molecular dynamics simulation. J. Mol. Model. 16, 789–798. https://doi.org/10.1007/s00894-009-0612-0.

Malik, A.R., Javed, M.K., Naved, A.A.M., 2017. Influence of antidepressant clomipramine hydrochloride drug on human serum albumin: Spectroscopic study. J. Mol. 241, 91–98.

Naik, P.N., Nandibewoor, S.T., Chimatadar, S.A., 2015. Non-covalent binding analysis of sulfamethoxazole to human serum albumin: Fluorescence spectroscopy, UV–vis, FT-IR, voltammetric and molecular modeling. J. Pharm. Anal. 5, 143–152. https://doi.org/10.1016/j.jpha.2015.01.003.

Nasser, A.A., Javed, M.K., Ajamaluddin, M., et al., 2020. Molecular interaction of tea catechin with bovine β-lactoglobulin: a spectroscopic and in silico studies. Saudi Pharm J. 28, 238–245.

Nusrat, S., Siddiqi, M.K., Zaman, M., et al., 2016. A comprehensive spectroscopic and computational investigation to probe the interaction of antineoplastic drug nordihydroguaiaretic acid with serum albumins. PloS One 11, e0158833. https://doi.org/10.1371/journal.pone.0158833.

Petitpas, I., Petersen, C.E., Ha, A.A., et al., 2003. Structural basis of albumin-thyroxine interactions and familial dysalbuminemic hyperthyroxinemia. Proc. Natl. Acad. Sci. 100, 6440–6445. https://doi.org/10.1073/pnas.1137188100.

Pan, X., Qin, P., Liu, R., Wang, J., 2011. Characterizing the interaction between tartrazine and two serum albumins by a hybrid spectroscopic approach. J. Agric. Food Chem. 59, 6650–6656. https://doi.org/10.1021/jf200907x.

Reichel, A., 2009. Addressing central nervous system (CNS) penetration in drug discovery: basics and implications of the evolving new concept. Chem. Biodivers. 6, 2030–2049. https://doi.org/10.1002/cbdv.200900103.

Rieko, I., 2015. Protein-Inhibitor Interaction Studies Using NMR. Appl NMR Spectrosc. 1, 143–181.

Ryan, M., Donald, J.J.B., Hage, D.S., 2015. Analysis of Drug-Protein Binding using On-Line Immunoextraction and High-Performance Affinity Microcolumns: Studies with Normal and Glycated Human Serum Albumin. J. Chromatogr. A 1416, 112–120.

Russell, B., Mulheran, P., Birch, D., Chen, Y., 2016. Probing the Sudlow binding site with warfarin: how does gold nanocluster growth alter human serum albumin?. PCCP 18, 22874–22878. https://doi.org/10.1039/c6cp03428d.

Sudlow, G., Birkett, D.J., Wade, D.N., 1976. Further characterization of specific drug binding sites on human serum albumin. Mol. Pharmacol. 12, 1052–1061.

Stephanos, J.J., 1996. Drug-protein interactions: two site binding of heterocyclic ligands to a monomeric hemogolobin. J. Inorg. Biochem. 62, 155–169. https://doi.org/10.1016/0162-0134(95)00144-1.

Simard, J.R., Zunszain, P.A., Hamilton, J.A., Curry, S., 2006. Location of high and low affinity fatty acid binding sites on human serum albumin revealed by NMR drug-competition analysis. J. Mol. Biol. 361, 336–351. https://doi.org/10.1016/j.jmb.2006.06.028.

Suryawanshi, D.V., Walekar, L.S., Gore, A.H., Anbhule, P.V., Kolekar, G.B., 2016. Spectroscopic analysis on the binding interaction of biologically active pyrimidine derivative with bovine serum albumin. J. Pharm. Anal. 6, 56–63. https://doi.org/10.1016/j.jpha.2015.07.001.

Trott, O., Olson, A.J., 2010. AutoDock Vina: improving the speed and accuracy of docking with a new scoring function, efficient optimization, and multithreading. J. Comput. Chem. 31, 455–561. https://doi.org/10.1002/jcc.21334.

Tayyab, S., Sam, S.E., Kabir, M.Z., Ridzwan, N.F., Mohamad, S.B., 2019. Molecular interaction study of an anticancer drug, ponatinib with human serum albumin using spectroscopic and molecular docking methods. Spectrochim. Acta A. 214, 199–206. https://doi.org/10.1016/j.saa.2019.02.028.

Valeur, B., 2001. Molecular Fluorescence: Principles and Applications. Wiley-VCH Press, NewYork.

Yang, A., Ma, M., Li, X., Xue, M., 2012. Interaction of irbesartan with bovine hemoglobin using spectroscopic techniques and molecular docking. J. Spectrosc. 27. https://doi.org/10.1155/2012/136287. Article ID 136287.

Zhong, W., Wang, Y., Yu, J.S., et al., 2004. The interaction of human serum albumin with a novel antidiabetic agent-SU-118. J. Pharm. Sci. 93, 1039–1046. https://doi.org/10.1002/jps.20005.

Zhou, X.-Q., Wang, B.-L., Kou, S.B., 2019. Multi-spectroscopic approaches combined with theoretical calculation to explore the intermolecular interaction of telmisartan with bovine serum albumin. Chem. Phys. 522, 285–293. https://doi.org/10.1016/j.chemphys.2019.03.019.

Zsila, F., 2013. Subdomain IB Is the third major drug binding region of human serum albumin: Toward the three-sites model. Mol. Pharm. 10, 1668–1682.